Journal of
Mechanics of
Materials and Structures

ANALYSIS OF STRESS-STRAIN DISTRIBUTION
WITHIN A SPINAL SEGMENT

Zdenka Sant, Marija Cauchi and Michelle Spiteri

Volume 7, No. 3 March 2012

msp

JOURNAL OF MECHANICS OF MATERIALS AND STRUCTURES
Vol. 7, No. 3, 2012
dx.doi.org/10.2140/jomms.2012.7.255

ANALYSIS OF STRESS-STRAIN DISTRIBUTION WITHIN A SPINAL SEGMENT

ZDENKA SANT, MARIJA CAUCHI AND MICHELLE SPITERI

The biomechanical feedback of biological tissue is difficult to measure. A spinal segment model can be used to obtain fundamental information by means of a computer simulation using finite element analysis.

1. Introduction

Interest in spine research has changed its focus from military-based tasks to problems related to the treatment of various spinal disorders, degenerative diseases, or traumas. Various studies have listed pain related to spinal structures as constituting the majority of health problems. A recent EU Commission study [EC 2007] also suggests that 67 million people suffered pain in their lower or upper back in the week previous to the survey.

The degenerative process accompanying aging causes changes in the form and composition of spinal tissues. This results in back pain particularly in cases such as internal disruption of the intervertebral disc (IVD) or stress shielding. In the case of stress shielding the damaged tissue has decreased ability to resist loading, and tends to be protected by adjacent healthy tissue, as occurs in the lumbar spine [Adams and Dolan 2005; Benzel 2005]. A healthy spine has nonlinear, elastic behavior and thus under lower loads provides little resistance while under increased loads it responds with augmented resistance. The stability of the spine provided by the IVD, the surrounding ligaments, and the muscles together with the geometry of the vertebral body must be preserved in any situation; thus in some cases a degenerated disc has to be replaced by an implant. Implant selection is usually based on the surgeon's own experience with particular implants and the results of tests carried out by the manufacturer in compliance with available standards. Unfortunately these results do not provide information about the biomechanical feedback which gives valuable insight for the surgeon. At the same time there is also a lack of information about the effect of degenerated components on the mechanical behavior of the entire IVD. Once the degenerative process alters the mechanical response, the whole complex structure of the segment is affected due to an adjustment of the load transfer trajectory that might affect as well the process of bone remodeling. All this might ultimately lead to undesirable performance of the IVD implant.

The goal of this work is to study the biomechanical behavior of a spinal segment under varying conditions related to the deterioration of the material properties of the IVD. Decisions about the methodology of this research and get satisfactory answers had to be made in the very early stages of the project. Since it is very difficult, if not impossible, to obtain the complete complex data about the response of different components of the system by means of measurements in vivo, and in the view that measurements in vitro

This research project was supported by grant 'R29' No. 31-329 obtained from the Research Fund Committee, University of Malta.

Keywords: spinal segment, finite element analysis, intervertebral disc.

are not feasible due to the lack of available spinal segments as well as economic and time constraints, the situation called for the development of a reliable computational model. Such a model would allow the investigation of biomechanical deficiencies within a geometrically identical pathological spinal segment and assist the proper understanding of the role played by each anatomical structure of the system.

2. Modeling

The pathophysiology of intervertebral disc degeneration is multifactorial [Hadjipavlou et al. 2008]. Mechanical factors have a significant effect, as excessive mechanical loading can cause disc structural disruption [Adams and Roughley 2006]. Disc degeneration impairs the shock-dissipating capacity of the vertebral column, thus a greater portion of the axial load is transmitted directly to the endplates of the lower adjacent vertebra [Norkin and Levangie 1992]. To provide a computational simulation of the desired situation, the creation of a computational model suitable for finite element analysis (FEA) was required.

The motion segment generated in this work consists of two adjacent vertebrae, L3 and L4, and an IVD modeled as a two-phase structure while the cartilages at the contact regions of the facet joints were simplified to a single-phase connective tissue. The material properties of the IVD, consisting of the annulus fibrosus (AF) and the nucleus pulposus (NP), distinguish the three different scenarios that simulate the physiological, the mildly degenerated IVD, and the fully degenerated IVD. Thus three spinal segments with different material properties simulated load transfer through a healthy IVD, a mildly degenerated IVD, and a severely degenerated IVD.

The two vertebrae were digitized using a reverse engineering approach applied to images in DICOM format, obtained from a computer tomography (CT) helical scan at Mater Dei Hospital. Each CT scan slide was processed by means of drawing software, capturing the real surface of the vertebrae with all anomalies, and the recreated vertebrae were then transported into the FEA package. To create the intervertebral disc we had to take into consideration the complexity of the real disc, the computational power required to sustain the simulation for such a complex structure, and the material data of [Acaroglu et al. 1995] based on an experimental investigation of the mechanical properties of anterior and posterior segments cut from the inner and outer layers of an AF. In the median plane, the lamellae reveal the major difference in their properties related to the posterior-anterior direction of their position. The collagenous fibers at the anterior median location are much stiffer than the lamellae found at the posterior side of the annulus, and both cases exhibit a nonlinear, axial stress-strain relation at low strains in "toe" region

	Young's modulus E (MPa)			
	Anterior		Posterior	
	Outer	Inner	Outer	Inner
Healthy annulus	27.2±14.6	7.6±6.6	13.6±9.4	2.4±2.5
Mild degeneration	23.3±16.6	6.1±5.2	6.6±4.0	4.3±4.9
Severe degeneration	21.2±12.2	4.8±4.5	8.2±5.5	3.4±3.9

Table 1. Young's modulus (mean ± standard deviation) in MPa for fibers at different locations of the annulus [Acaroglu et al. 1995].

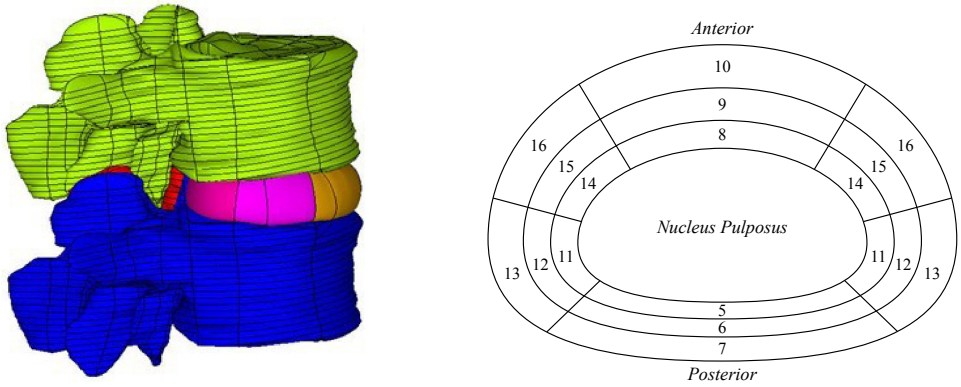

Figure 1. Spinal segment L3-L4 with detail of IVD model.

while at the region of high strains the behavior is nearly linear. The Young's modulus, as a result of a cubic function fitted to the experimental data, is presented in Table 1 as continuously varying from the posterior to the anterior side of the annulus [Acaroglu et al. 1995].

Our model of the IVD in Figure 1 represents a simplification of an IVD that in reality has 10–20 layers of collagen fibers encapsulating the nucleus. The NP was modeled as a single volume surrounded by three lamellae divided into six segments. Further connective tissue was created at the region of the facet joints. Considering that the loads applied to the bone would result in bone response, which can be approximated by a linear function, the two types of bone tissue, cortical and cancellous, were modeled as linear isotropic material even though in reality the bone is anisotropic heterogeneous viscoelastic material. The necessity for simplification is related to the computational power and CPU time required for the simulation, together with the available geometry/material data and modeling facility. The continuously changing directions of trabeculae orientation within both types of bone tissue are compensated for by the corresponding orientation of the elements within each structure. Thus, accepting these simplifications, the verified data of the Young's modulus for the cortical bone, the cancellous bone, and the endplates was used as listed in Table 2. The material properties of the IVD were extrapolated from available data [Acaroglu et al. 1995] and processed using (2-1) to evaluate the Young's modulus/Poisson's ratio at the geometrical positions of the outer and inner locations of the segment. The average value of the Young's modulus/Poisson's ratio was then computed using (2-2). The computation was based on the assumption of linear variation of both quantities in the sagittal and transverse directions:

$$E_{sl} = \frac{E_{jo} - E_{ji}}{d_{jl}} * d_{sl}, \tag{2-1}$$

Material properties of vertebrae			
Component	Young's modulus (MPa)	Poisson's ratio	Reference
Cortical bone	16000	0.25	[Sant 2007]
Cancellous bone	120	0.25	[Sant 2007]
Endplate	500	0.25	[Teo et al. 2003]

Table 2. Material properties of vertebrae.

	Material properties of IVD			
	Healthy IVD		Severely degenerated IVD	
	E (MPa)	ν	E (MPa)	ν
NP	100	0.499	1	0.499
AF 5	6.75	0.445	2.25	0.345
AF 6	9.75	0.425	3.25	0.325
AF 7	13.5	0.4	4.5	0.3
AF 8	9.5	0.415	5	0.315
AF 9	15.5	0.395	9	0.295
AF 10	23	0.37	14	0.27
AF 11	7.575	0.436	3.075	0.336
AF 12	11.475	0.416	4.975	0.316
AF 13	16.35	0.391	7.35	0.291
AF 14	8.675	0.424	4.175	0.324
AF 15	13.775	0.404	7.275	0.304
AF 16	20.15	0.379	11.15	0.279

Table 3. Computed material properties of IVD based on data from [Acaroglu et al. 1995].

where E_{jo}, E_{ji}, and E_{sl} represent the Young's moduli at the outer j position, the inner j position, and the position defined by d_{sl}, respectively, and d_{jl} and d_{sl} represent the distances l between the outer and inner j position and between the segment's position and the outer j reference position, respectively. The average value used in our simulation for segment s is computed from

$$E_{av_s} = \frac{E_{jo} + E_{sl}}{2}. \tag{2-2}$$

The material properties characterizing the healthy and degenerated states of the IVD material are listed in Table 3 according to the position of each AF segment.

Finally, the discretization of the virtual solid model was created by means of combination of free and mapped meshing using an esize of two elements. The cortical bone and endplates were meshed with shell elements having bending and membrane capabilities while the cancellous bone was meshed with a solid element type with midside nodes. The connectivity between various meshes at the contacting surfaces between the vertebrae and the IVD was secured through the use of contact elements, which were set to "always bonded contact". Another pair of contact surfaces set to "standard contact condition" were created at the facet joints to allow for flexion/extension movement and limited torsion, as well as to provide resistance to the sliding of the vertebrae against each other.

3. Simulation

In addition to the geometrical and material model, the FE model in Figure 2 also requires the load model. The latter depends on the particular activity associated with the certain position on the spine, which is in turn associated with a particular load transfer through the spinal structure. The spine undergoes a combined motion due to the fact that simple flexion is always accompanied by coupled motions, which

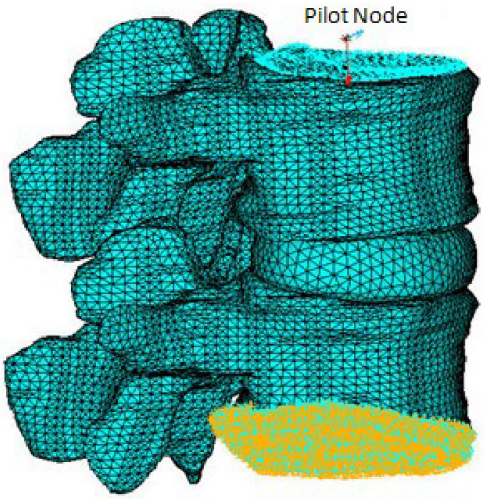

Figure 2. Finite element model of the spinal segment L3-L4.

vary in nature and magnitude according to the level of the segment within the whole spine. Thus the applied load simulating physiological activity can be either in the form of displacement and rotation or forces and moments. Due to the fact that the model in this study was simplified and therefore did not include any ligamentous structures, the exact neutral range of motion for the L3-L4 segment must be applied to simulate a real life situation without the contribution of the ligamentous structures to the load transfer. Since this data was not available, it was decided to run the simulation based on [Arjmand and Shirazi-Adl 2006], in which the authors measured and verified data for the lumbar spine at various positions without contribution from ligamentous structures. Such data was deemed suitable for the simulation in the present study. The simulated load for various positions of the patient was comprised of the compressive force, shear force, and bending moment. It was decided to simulate an upright standing position without additional external carrying load from the hands. In this situation, the sagittal moment $M = 3.9\,\text{Nm}$ is positive while the segment is in flexion, the axial compression $N = 447\,\text{N}$, and the shear force $S = -63\,\text{N}$ is positive in the anterior direction. These loads were applied by means of a pilot node positioned at the fictitious midplane in the center of the NP of the intervertebral disc L2-L3. This corresponds to the position where the data was measured and computed by Arjmand and Shirazi-Adl. By having identical geometry and loading conditions, it was possible to run a comparative analysis in order to investigate the effect of IVD degeneration on the mechanical behavior of the segment. Thus the simulation was performed for three different conditions: physiological, mildly degenerated IVD, and severely degenerated IVD.

4. Results

The comparative study presented here aims to investigate the effect of pathological deterioration of the material properties on the load transfer through the IVD and the biomechanical feedback of the adjacent structures. To be able to correctly analyze and compare the results, the necessary path passing throughout the median plane of the segment at the center of the nucleus had to be created. The results in the

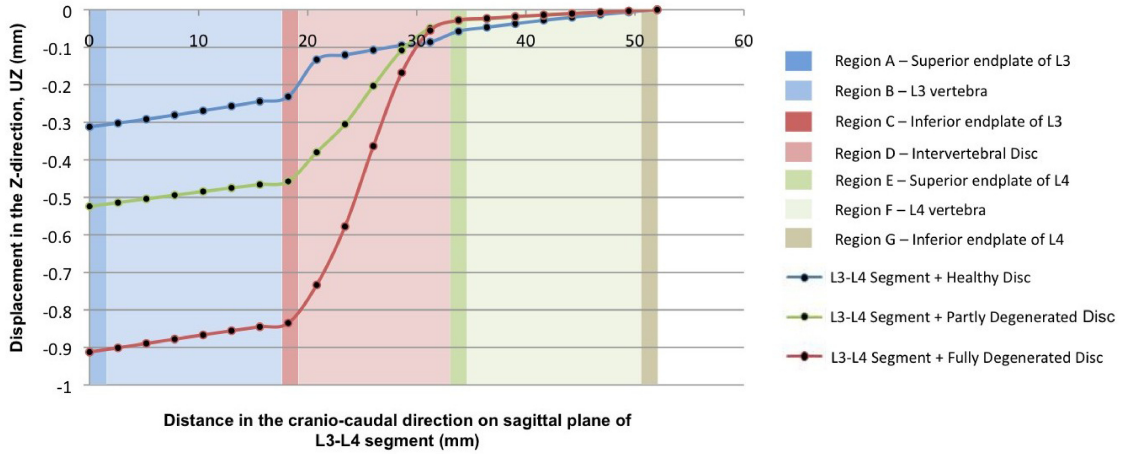

Figure 3. Variation of displacement along the craniocaudal direction for L3-L4 segment.

craniocaudal direction for both the vertebrae and the IVD were mapped onto this path. These results are visualized in Figure 3, from which the effect of degeneration on the mechanical behavior was then analyzed. The gradients in Figure 3 correspond to the relative stiffness/Young's modulus of the entity, thus the greater gradient implies a lower Young's modulus and therefore a higher deformation ability. It is the IVD that always deforms the most irrespective of the state of degeneration, as confirmed by the steeper gradients within the IVD region (region D) when compared to the gradients through the L3 and L4 vertebrae represented by regions B and F, respectively. The larger displacement of the fully degenerated IVD consequently causes the segment to undergo larger displacement. In regions C and E the gradient is shallower due to the stiffening effect of the vertebral endplates. The main biomechanical deficiency of the partly and fully degenerated IVD is the inability to properly transfer the load between adjacent vertebrae as a direct consequence of the reduced stiffness and lax behavior. Thus in the cases of the partly and fully degenerated IVD, the inferior vertebra undergoes a smaller axial displacement than in the case of the healthy disc since the degenerated NP within the degenerated IVD lacks the necessary mechanical properties to bulge into the endplate of the inferior vertebra while the spinal segment is loaded, and thus it does not transmit the load properly through the segment. The axial displacement approaches zero on proceeding along the craniocaudal direction since the bottom surface of the inferior vertebra was fully constrained to be able to run the computational task.

The cortical bone is the main bearer of the load, from where the load is subsequently redistributed to the cancellous bone which fulfils the role of a shock absorber. Thus the highest compressive stresses, represented by the third principal stress, were developed at the level of the cortical bone in the posterior region of the vertebrae mainly around the pedicles in the case of the healthy IVD, as shown in Figure 4a, while in the case of the severely degenerated IVD, shown in Figure 4b, the maximum compressive stress developed at the anterior region of the epiphyseal ring. It can be noticed that the overall compressive stresses increased from 12 MPa in the case of the healthy IVD to 22.5 MPa in the case of the degenerated IVD. The cancellous bone functioning as a shock absorber develops the highest compressive stress just beneath the vertebral endplates. It is clinically confirmed that the site of the most frequent failures due to compressive loading is the region of the endplates. The cancellous bone beneath the healthy disc in

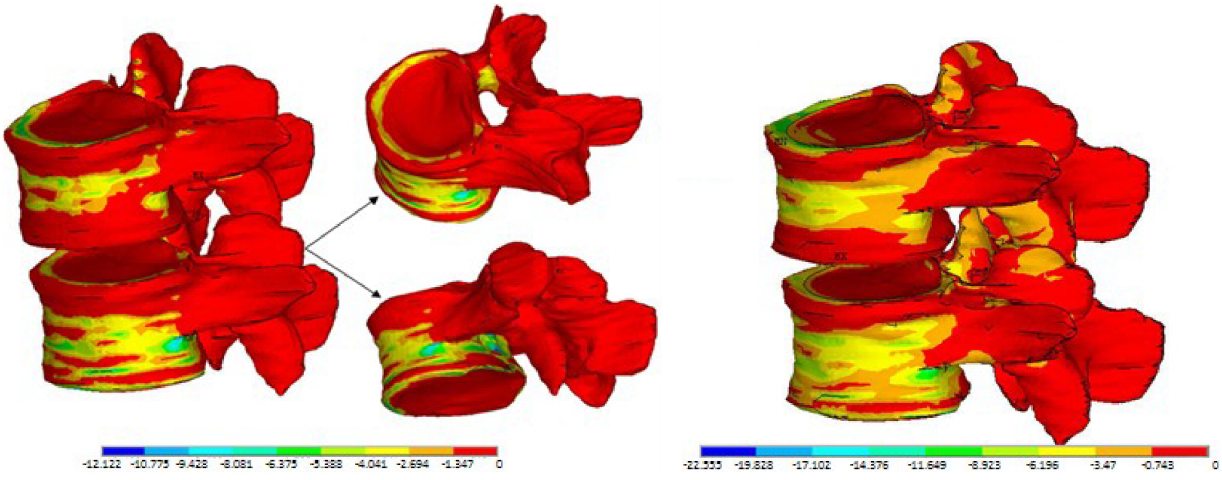

(a) (b)

Figure 4. Variation of third principal compressive stress within the cortical bone for L3-L4 segment.

Figure 5a is subjected to larger compressive stresses than the cancellous bone beneath the severely degenerated IVD in Figure 5b, which indicates that, due to reduced stiffness, the degenerated IVD undergoes larger deformation radially, and thus reduces the load transferred through the superior endplate of the inferior vertebra. Thus the cancellous bone is characterized by lower compressive stresses, indicating a reduced magnitude of disc bulging into the endplate in the case of the severely degenerated disc, which increases the compressive stress within the cancellous bone from 1.034 MPa to 1.328 MPa for the healthy and severely degenerate IVD, respectively. The maximum tensile stress increased as well, from 0.039 MPa for the healthy IVD to 0.117 MPa for the severely degenerated IVD. The full analysis

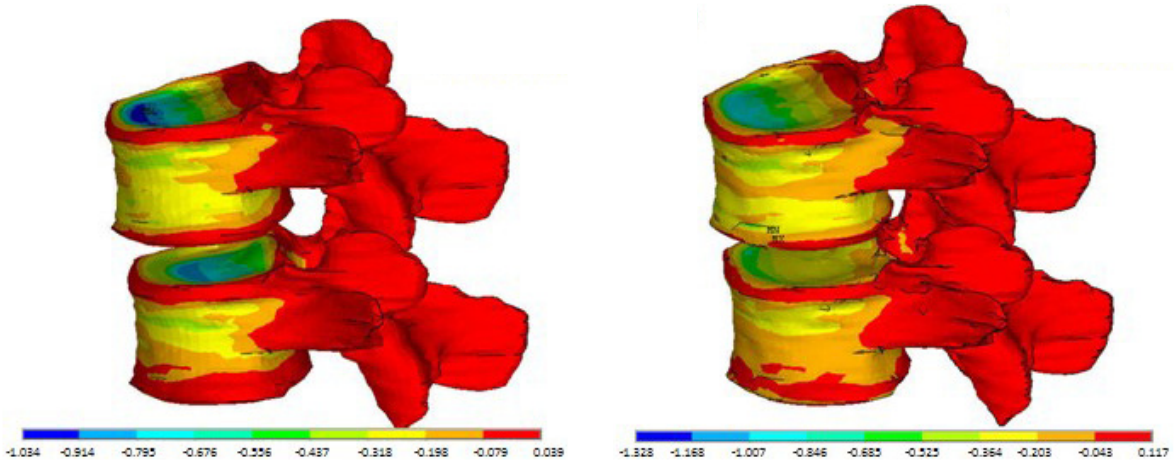

(a) (b)

Figure 5. Variation of third principal compressive stress within the cancellous bone for L3-L4 segment.

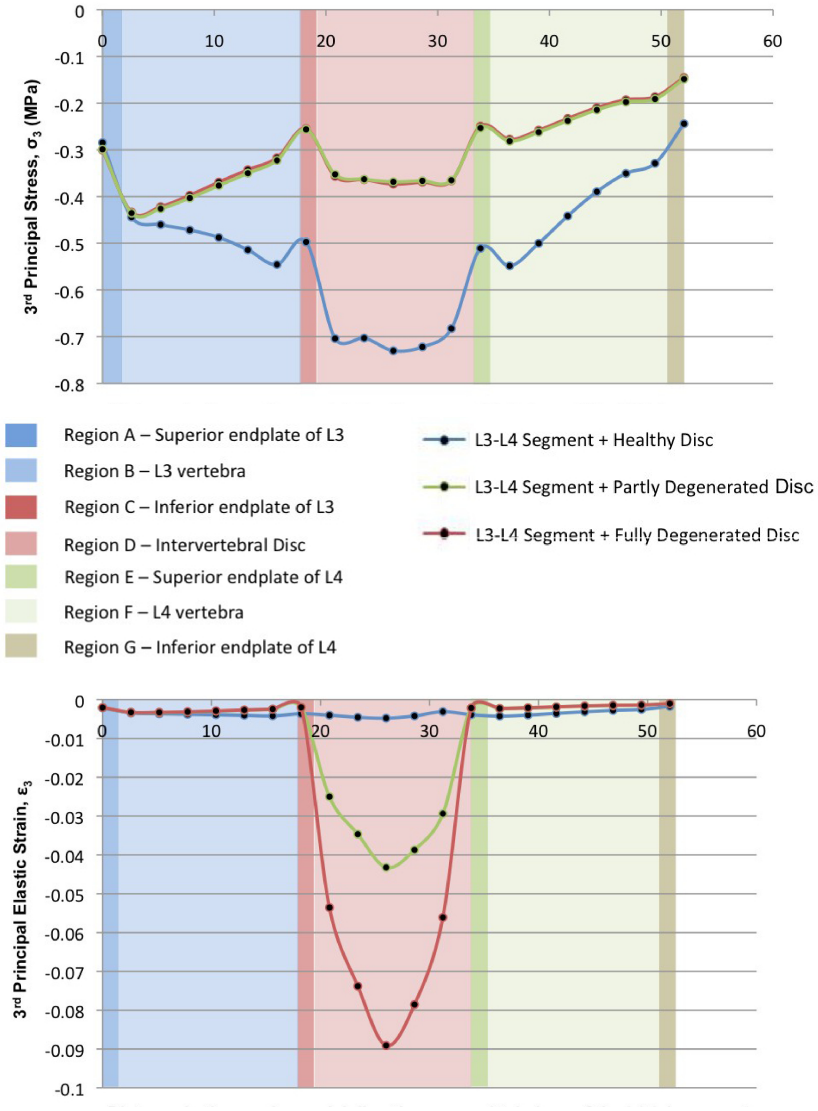

Figure 6. Variation of stress-strain along the central path in the craniocaudal direction for L3-L4 segment. The horizontal axis represents distance in mm.

of the biomechanical feedback due to the degenerative process is summarized by the graphs in Figure 6 representing the stress and strain variation along the axial craniocaudal direction through the center of the spinal segment.

5. Conclusion

These results, together with others in the posterior-anterior and lateral directions, were verified by the clinician and carefully analyzed. In all cases, the importance of the endplates and the effect of the degeneration of the nucleus were confirmed. The virtual FE model can be used for other simulations

such as the effect of loading on the biomechanical feedback of the spinal segment, in particular the structures forming the intervertebral disc, and the effect of different physical activities on load transfer through the segment.

References

[Acaroglu et al. 1995] E. R. Acaroglu, J. C. Latridis, L. A. Setton, R. J. Foster, V. C. Mow, and M. Weidenbaum, "Degeneration and aging affect the tensile behavior of human lumbar annulus fibrosus", *Spine* **20**:24 (1995), 2690–2701.

[Adams and Dolan 2005] M. A. Adams and P. Dolan, "Spine biomechanics", *J. Biomech.* **38**:10 (2005), 1972–1983.

[Adams and Roughley 2006] M. A. Adams and P. J. Roughley, "What is intervertebral disc degeneration, and what causes it?", *Spine* **31**:18 (2006), 2151–2161.

[Arjmand and Shirazi-Adl 2006] N. Arjmand and A. Shirazi-Adl, "Model and in vivo studies on human trunk load partitioning and stability in isometric forward flexions", *J. Biomech.* **39**:3 (2006), 510–521.

[Benzel 2005] E. C. Benzel (editor), *Spine surgery: techniques, complication avoidance, and management*, Churchill Livingstone, Philadelphia, 2005.

[EC 2007] *Health in the European Union*, Special Eurobarometer 272e, European Commission, 2007, Available at http://ec.europa.eu/health/archive/ph_publication/eb_health_en.pdf.

[Hadjipavlou et al. 2008] A. G. Hadjipavlou, M. N. Tzermiadianos, N. Bogduk, and M. R. Zindrick, "The pathophysiology of disc degeneration: a critical review", *J. Bone Jt. Surg. Br.* **90**:10 (2008), 1261–1270.

[Norkin and Levangie 1992] C. C. Norkin and P. K. Levangie, *Joint structure and function: a comprehensive analysis*, 2nd ed., Davis, Philadelphia, 1992.

[Sant 2007] Z. Sant, *Mechanické vlastnosti hrudního a bederního páteřního fixátoru*, Ph.D. thesis, University of Technology, Brno, 2007. Scientific Writings of the Technical University in Brno **446**.

[Teo et al. 2003] E. C. Teo, K. K. Lee, H. W. Ng, T. X. Qui, and K. Yang, "Determination of load transmission and contact force at facet joints of L2–L3 motion segment using FE method", *J. Musculoskelet. Res.* **7**:2 (2003), 97–109.

Received 14 Oct 2010. Revised 20 Jul 2011. Accepted 15 Dec 2011.

ZDENKA SANT: zdenka.sant@um.edu.mt
Mechanical Engineering Department, University of Malta, Tal Qroqq, Msida MSD 2080, Malta

MARIJA CAUCHI: mcau0010@um.edu.mt
Mechanical Engineering Department, University of Malta, Tal Qroqq, Msida MSD 2080, Malta

MICHELLE SPITERI: michespi@gmail.com
Mater Dei Hospital, Tal Qroqq, Msida MSD 2080, Malta

JOURNAL OF MECHANICS OF MATERIALS AND STRUCTURES

jomms.net

Founded by Charles R. Steele and Marie-Louise Steele

See http://jomms.net for submission guidelines.

JoMMS (ISSN 1559-3959) is published in 10 issues a year. The subscription price for 2012 is US $555/year for the electronic version, and $735/year (+$60 shipping outside the US) for print and electronic. Subscriptions, requests for back issues, and changes of address should be sent to Mathematical Sciences Publishers, Department of Mathematics, University of California, Berkeley, CA 94720–3840.

JoMMS peer-review and production is managed by EditFLOW® from Mathematical Sciences Publishers.

PUBLISHED BY

mathematical sciences publishers

http://msp.org/

A NON-PROFIT CORPORATION

Typeset in LaTeX

Journal of Mechanics of Materials and Structures

Volume 7, No. 3 March 2012

Special issue

Trends in Continuum Physics (TRECOP 2010)

1559-3959(2012)7:3;1-B